Electron-phonon interactions in the superconducting Chevrel phase compounds $Mo_6Se_{8-x}S_x$

Masafumi Furuyama,* Norio Kobayashi, and Yoshio Muto
Institute for Materials Research, Tohoku University, Katahira 2-1-1, Sendai 980, Japan
(Received 12 April 1989)

The specific heat of nine single crystals of the Chevrel phase compounds $Mo_6Se_{8-x}S_x$ ($0 \leq x \leq 4.0$) has been investigated in the temperature range 1.5–9.0 K in magnetic fields of 0 and 6 T. Using the BCS theory with strong-coupling corrections, the thermodynamic properties and information on the electron-phonon interactions have been obtained. The superconducting transition temperatures T_c of these compounds decrease with increasing S concentration x, and the electron-phonon interactions of this system change from strong to weak. In spite of the change in T_c, the bare electronic density of states is nearly constant for all samples. The value of T_c depends on the average phonon frequency through the electron-phonon coupling constant. The anomalous lattice specific heat has been observed for low concentration samples. This is explained by assuming low-lying soft-phonon modes, which were reported by inelastic neutron experiments for Mo_6Se_8, in addition to a molecular crystal model. The relationship between the electron-phonon interactions and the low-lying soft-phonon modes is discussed.

I. INTRODUCTION

The ternary molybdenum chalcogenides (Chevrel phase compounds) have been studied considerably because they have the highest upper critical magnetic field H_{c2} (Ref. 1) and relatively high superconducting transition temperatures T_c (Ref. 2) before the discoveries of the new high-T_c oxide superconductors. These compounds have compositions $M_X Mo_6X_8$ or Mo_6X_8, where M is a metal atom and X is a chalcogen atom. By analyzing the results of the specific-heat studies on a large number of the Chevrel phase compounds, pure ternary MMo_6X_8 and pure binary Mo_6X_8, where "pure" means X is not an alloy but an element, Lachal *et al.*[3] concluded that the strength of the electron-phonon coupling and then the superconducting transition temperatures of these compounds are dominated by the band electronic density of states.

On the other hand, for pseudoternary $MMo_6X_{8-x}X'_x$ and pseudobinary $Mo_6X_{8-x}X'_x$ compounds, such a relationship between the electron-phonon coupling constant and the band density of states does not always hold. Sankaranarayanan *et al.*[4] observed that the superconducting transition temperature for $Cu_{1.8}Mo_6S_{8-x}Se_x$ and $Cu_{1.8}Mo_6S_{8-x}Te_x$ decreases with increasing residual resistivity. Maekawa and Fukuyama[5] and Anderson *et al.*[6] pointed out the localization effect suppressed the superconducting transition temperature by increasing the effective Coulomb repulsion. These theoretical predictions may explain the experimental results of Sankaranarayanan *et al.*[4] because the localization effect also reduces the electrical conductivity of materials.

The lattice dynamics of the Chevrel phase compounds was studied in the framework of a simple molecular crystal model proposed by Bader *et al.*[7] In this model, the compound is regarded as a molecular crystal which consists of M atoms and quasirigid Mo_6X_8 units. The lattice dynamics then is simplified. The 45 normal modes of the unit cell are grouped into 36 internal modes of the Mo_6X_8 clusters and nine external modes: three acoustic and three optical modes associated with the M atoms and the clusters and three torsional modes of the clusters. The generalized phonon density of states obtained from the neutron experiments by Bader *et al.*[7] and Schweiss *et al.*[8] were qualitatively explained by this model.

Culetto and Pobell[9] analyzed their isotope experiment in Mo_6Se_8 using the molecular crystal model and pointed out the contribution of the translational acoustic modes and the internal modes to its superconductivity. By comparing the tunneling data on $Cu_{1.8}Mo_6S_8$ and $PbMo_6S_8$ with the generalized phonon density of states, Poppe and Wühl[10] showed that both low-frequency external modes and high-frequency internal modes coupled to the electron, while the optical modes associated with M atoms are ineffective to the electron-phonon coupling.

We[11] reported the result of the specific-heat measurement of Me_6Se_8 and pointed out that this compound is a strong-coupling superconductor on the basis of its thermodynamic properties. We also suggested that the low-energy phonon modes play an important role in its superconductivity. In the "alloyed" compounds $Mo_6Se_{8-x}S_x$ the substitution of the atoms in the cluster may cause the change of the lattice dynamics. Therefore, it is interesting to examine the relationship between the phonon characters and superconductivity in alloyed compounds.

In the present paper, we give the results of the specific-heat measurements on nine pseudobinary $Mo_6Se_{8-x}S_x$ single crystals, together with the results of tunneling spectroscopy in Mo_6Se_8 and $Mo_6Se_7S_1$. The thermodynamic properties, the electron-phonon interactions, and a phonon-softening effect which appeared in the present pseudobinary system are discussed in detail.

II. EXPERIMENT

Nine single crystals with the formula $Mo_6Se_{8-x}S_x$ ($x=0$, 0.2, 0.5, 0.7, 1.0, 1.5, 2.0, 3.0, 4.0) were prepared as follows. Only samples with concentrations of x smaller than 4.0 were possible to synthesize.[12] Powders of Mo, Se, and S, about 15 g in total, were mixed and pressed into a pellet and reacted three times at about 1100–1300 °C for 24–70 h in an evacuated quartz capsule. After the heat treatment, the powdered sample was melted in an induction furnace at about 1800–1850 °C under the Ar or He pressure of about 20–50 bars in an alumina crucible. Single crystals with sizes about $3\times2\times2$ mm^3 were obtained by use of the Stockberger-Bridgman technique. The samples had (100) cleaved surfaces confirmed by a back-Laue reflection technique.

The specific heat of all the samples was measured in the temperature range 1.5–9 K in the absence of a magnetic field as well as in a magnetic field of 6 T. Because of rather small samples, a thermal relaxation technique was used as described elsewhere.[13] The electronic tunneling spectroscopy was done by a point-contact method using a Zn-doped GaAs tip with a carrier concentration of 2.3×10^{19}/cm^3. The probe was prepared using a technique described in detail in Ref. 14. This probe was pressed onto the cleaved surface of the sample by a mechanically screw-driven apparatus. The usual method was used for the I versus V and dV/dI versus V measurements.[15] Our measuring system was calibrated by the characteristic measurements of the superconducting Pb and In samples.

III. RESULTS

Figures 1(a)–1(i) show the results of the specific-heat measurements in the form C/T versus T^2 under magnetic fields 0 and 6 T for samples with $x=0$, 0.2, 0.5, 0.7, 1.0, 1.5, 2.0, 3.0, and 4.0, respectively.

It should be noticed in Fig. 1 that the normal-state specific heat shows strong deviations from the Debye T^3 law for samples with the small concentration x. These deviations have also been reported in many Chevrel phase compounds.[3,16]

The following polynomial expression is used for the analyses of specific-heat results:

$$C_n(T)=\gamma T+\beta T^3+\alpha T^5 . \quad (1)$$

The parameters γ, β, and α are estimated by a least-squares method and are listed in Table I. The coefficient α, representing the anomalous T^5 term, is negative and depends upon the concentration x for $x\leq1.5$, while $\alpha\sim0$ for $x\geq2.0$. This anomalous specific heat may be caused by the phonon anomaly which was measured by the inelastic neutron-scattering experiments for Mo_6Se_8 (Ref. 8), as discussed in Sec. IV.

The superconducting transition temperatures T_c except $x=4.0$ were defined as the temperatures at which entropies of the superconducting and normal states become equal, while T_c for the sample with $x=4.0$ could not be determined by the specific-heat measurements, as seen in Fig. 1(i). Entropies of both states were numerically calculated from the equation, $S(T)=\int_0^T dT'C(T')/T'$. The normal-state specific heat, $C_n(T)$, was fitted by using Eq. (1). The smoothed curve for the specific heat of the superconducting state $C_s(T)$ was drawn in the temperature range of $1.5<T<T_c$. Below 1.5 K, the exponentially extrapolated curve and the curve extrapolated by T^3 were used for $x\leq1.5$ and $x\geq2.0$, respectively. Each T_c falls within the transition width ΔT_c which is defined as the temperature difference between the top and bottom of the specific-heat jump. The values of ΔT_c are less than 0.4 K in all cases except $x=4.0$. The values of T_c defined from the specific-heat measurements agree with those determined by electrical resistivity measurements. For $x=4.0$, T_c was determined by an electrical resistivity measurement. The concentration dependence of T_c is shown in Fig. 2 and is also listed in Table I. This dependence is nearly in agreement with that measured on sintered samples reported by Chevrel *et al.*[12] The chemical concentration analyses of the single-crystal samples have not been done. However, the agreement of T_c with sintered samples[12] and the sharp superconducting transition in the specific heat would permit us to use the nominal concentration values for our single crystals.

The thermodynamic critical magnetic field $H_c(T)$ is estimated from the difference of $C_n(T)$ and $C_s(T)$ as follows:

$$VH_c(T)^2/8\pi=\int_T^{T_c}dT'\int_{T'}^{T_c}dT''[C_s(T'')/T''-C_n(T'')/T''] , \quad (2)$$

TABLE I. Superconducting transition temperature T_c which was obtained from the specific-heat measurements for $x\leq3.0$ and from the electrical resistivity measurement for $x=4.0$, and the coefficients for the normal-state specific heat, $C_n(T)=\gamma T+\beta T^3+\alpha T^5$.

x	0.0	0.2	0.5	0.7	1.0	1.5	2.0	3.0	4.0
T_c (K)	6.34	5.49	4.95	4.68	4.56	3.75	2.94	2.59	1.86
γ (mJ/mol K^2)	47.2	46.9	45.7	45.6	45.1	38.8	37.8	35.1	32.3
β (mJ/mol K^4)	3.65	3.11	2.72	2.65	2.40	2.26	1.70	1.69	1.24
$-\alpha$ (10^{-2} mJ/mol K^6)	1.06	0.58	0.40	0.45	0.46	0.25	0.0	0.0	0.0

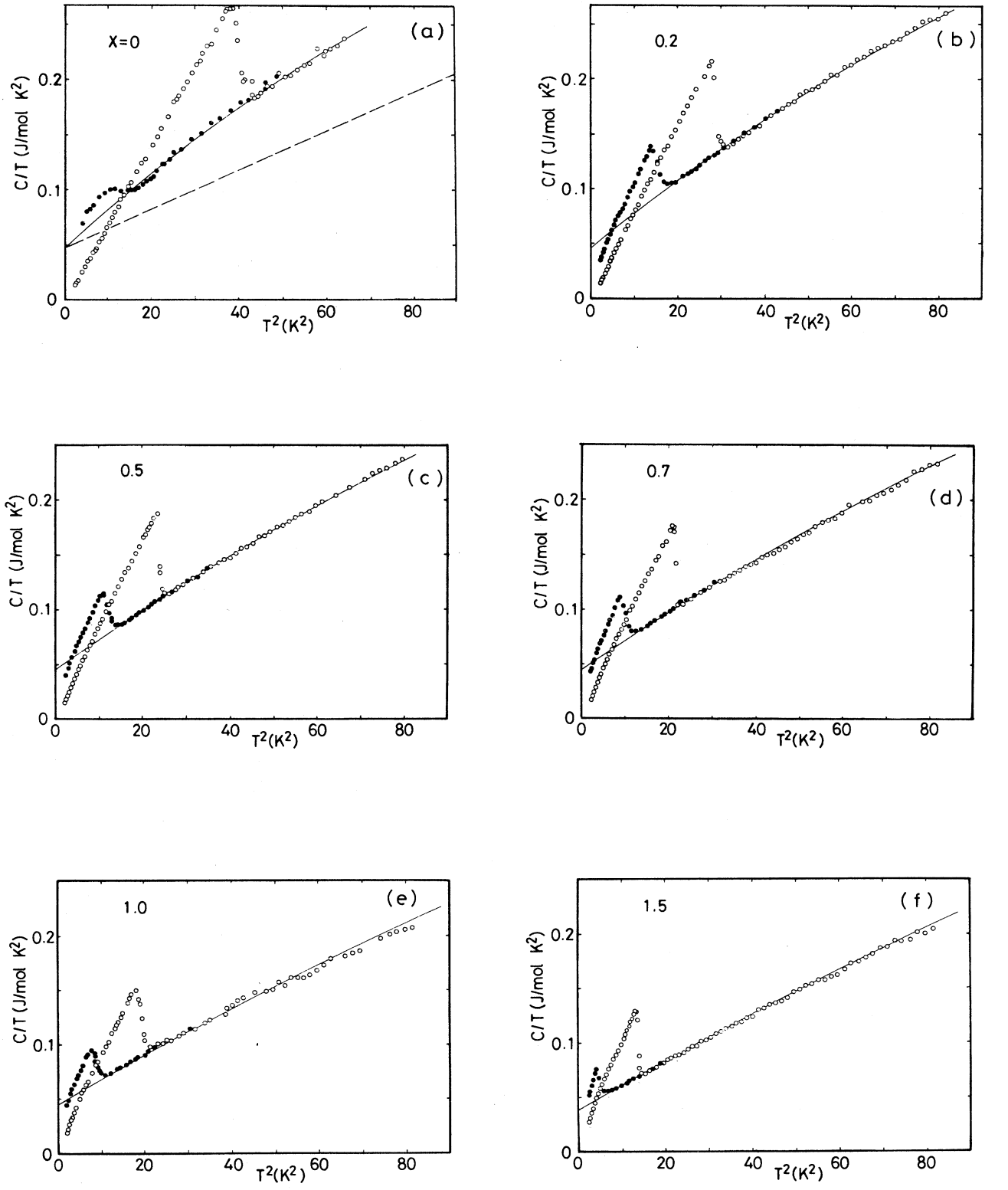

FIG. 1. (a)–(i). Low-temperature specific heat plotted as C/T vs T^2. Open and closed circles represent the results at 0 and 6 T, respectively. Solid lines are calculated from our phonon model including the low-lying soft-phonon modes and dashed line in (a) from only three acoustic modes excluding low-lying phonon ones.

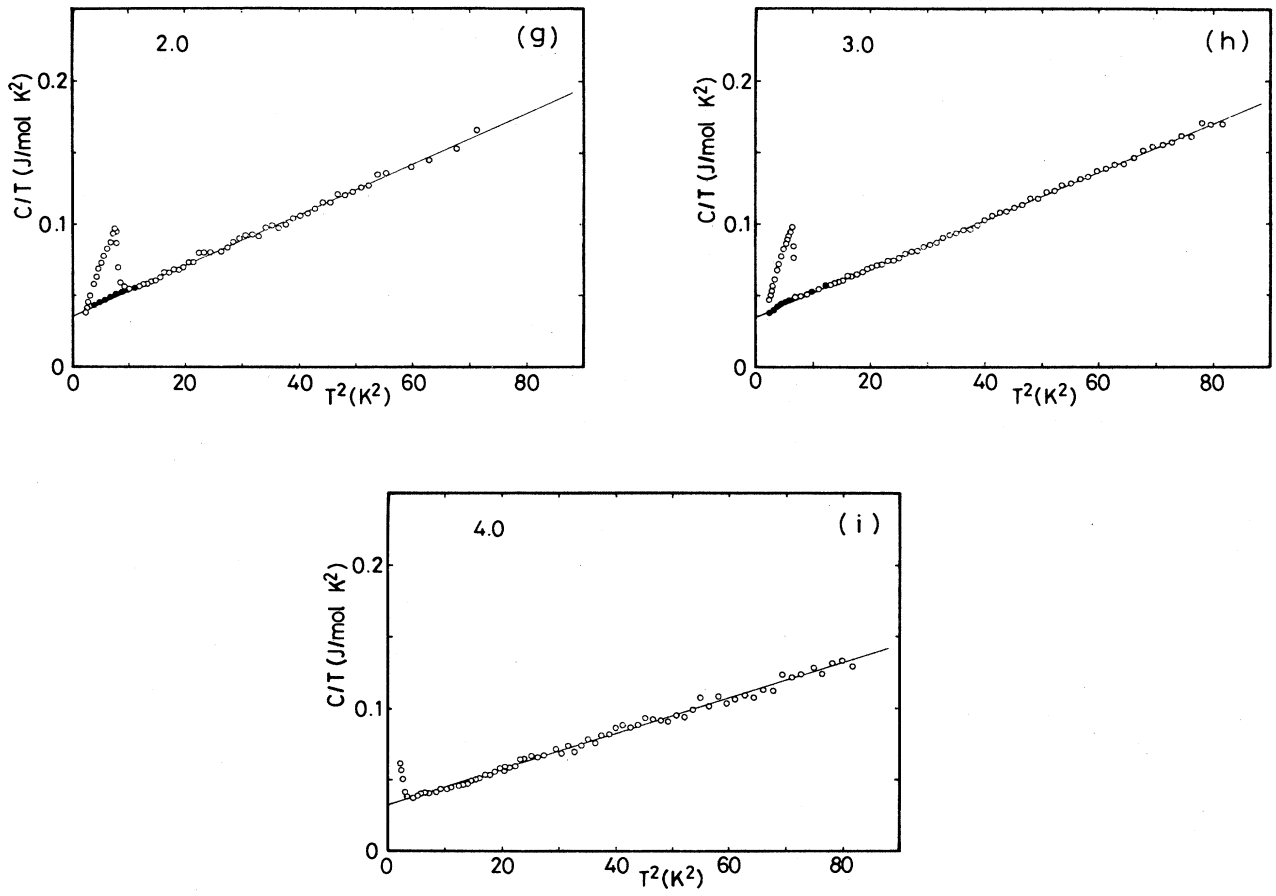

FIG. 1. (*Continued*).

where V is a molar volume. In Table II, the values of $H_c(0)$ and the slope at T_c, $-dH_c/dT$, are listed. The validity of this procedure is examined by comparing $(dH_c/dT)_{T_c}$ obtained with the value estimated from the Rutgers equation,

$$(dH_c/dT)^2_{T_c} V/4\pi = \Delta C/T_c \ , \tag{3}$$

where ΔC is a specific heat jump at T_c. The values of $(dH_c/dT)_{T_c}$ estimated from ΔC are also listed in Table II. Good agreements between these values are obtained for $x \leq 1.5$. Slightly larger discrepancies, however, are noticeable for $x = 2.0$ and 3.0, and these discrepancies may be caused by the difficulty of the extrapolation of $C_s(T)$ to 0 K.

TABLE II. Thermodynamic quantities.

x	0.0	0.2	0.5	0.7	1.0	1.5	2.0	3.0
$\Delta C(T_c)$[a] (mJ/mol K)	682	560	407	371	346	250	158	139
$H_c(0)$[a] (10^{-4} T)	849	719	619	585	568	438	301	271
$-(dH_c/dT)_{T_c}$[a] (10^{-4} T/K)	275	262	237	237	228	214	190	187
$-(dH_c/dT)_{T_c}$[b] (10^{-4} T/K)	276	267	241	237	232	219	197	198

[a]Direct analyses.
[b]From Rutgers relation.

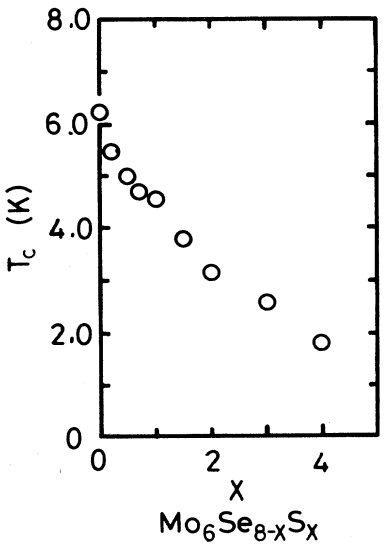

FIG. 2. Concentration dependence of T_c.

Four important thermodynamic values to characterize the superconductor, $\Delta C/\gamma T_c$, $H_c(0)^2/\gamma T_c^2$, $-(dh_c/dt)_1$, and $D(t)$, are derived from the specific-heat measurements, where $h_c(t)$ $[=H_c(T)/H_c(0)]$ is the normalized thermodynamic critical magnetic field, t is the normalized temperature, and $D(t)$ the deviation of $h_c(t)$ from the parabolic law, $D(t)=h_c(t)-(1-t^2)$. The concentration dependences of the thermodynamic parameters, $\Delta C/\gamma T_c$, $H_c(0)^2/\gamma T_c^2$, and $-(dh_c/dt)_1$ are shown in Figs. 3(a), 3(b), and 3(c), respectively. The respective Bardeen-Cooper-Schrieffer (BCS) values are 1.43, 5.95, and 1.73 and are indicated by dashed lines in figures. The t^2 dependences of $D(t)$ are shown in Fig. 4, where $D(t)$ in the BCS theory is also shown in this figure together with data of Pb.[17] $\Delta C/\gamma T_c$ and $-(dh_c/dt)_1$ represent the property of the superconducting state at T_c and $H_c(t)^2/\gamma T_c^2$ at 0 K. On the other hand, $D(t)$ represents the superconducting property over the temperature range from zero to T_c. All of these parameters, however, show the following trend in the concentration dependence: For smaller x, the values of the parameters deviate strongly from the BCS values. As the concentration x increases, these deviations become smaller and the values of the parameters approach the BCS values. This behavior indicates that this system changes from a strong-coupling superconductivity to a weak-coupling one as the concentration x increases.

The energy gap is also estimated from the electronic specific heat of the superconducting state C_{ES} by use of the "α model" proposed by Padamsee *et al.*[18] They treated the quasiparticles in the excited states as well-defined fermions, and described the entropy of the superconducting state S_{ES} by the expression

$$S_{ES}=-2k_B\sum_k[f_k\ln f_k+(1-f_k)\ln(1-f_k)]\ ,$$

where k_B is Boltzmann constant and f_k is the Fermi dis-

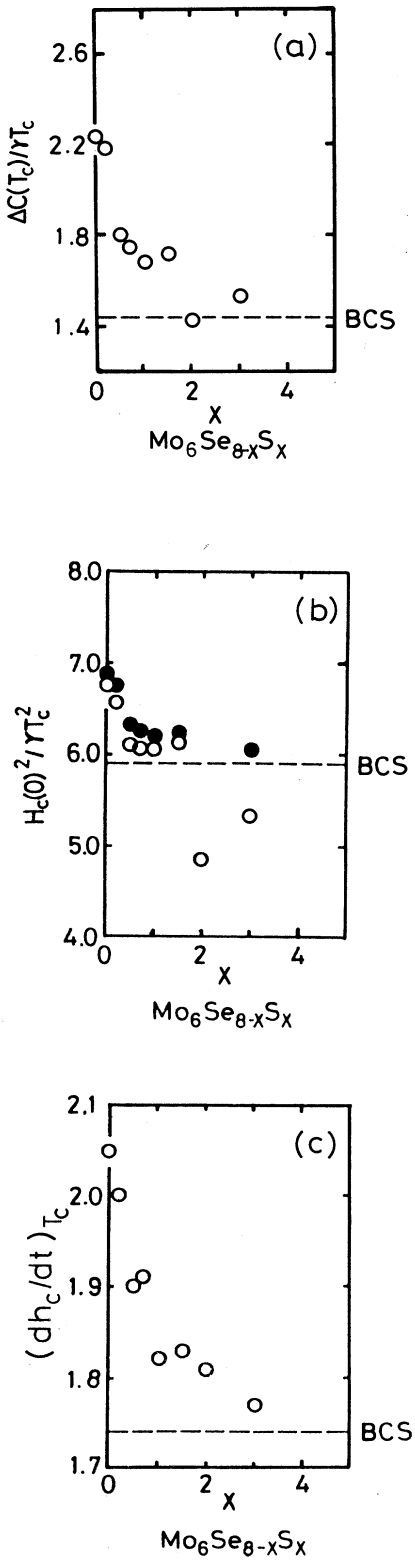

FIG. 3. Concentration dependence of the thermodynamic quantities. Open circles are experimental values and the dashed line shows the BCS value. (a) $\Delta C/\gamma T_c$, (b) $H_c(0)^2/\gamma T_c^2$, and (c) $-(dh_c/dt)_1$. Closed circles are derived from Eq. (6).

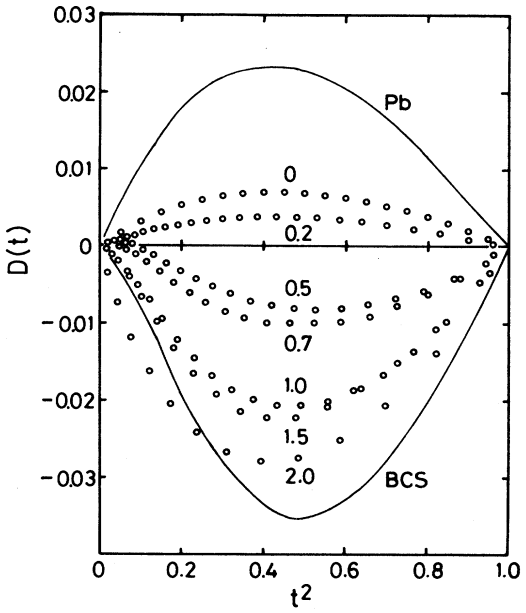

FIG. 4. Deviation $D(t)$ from the parabolic law of $H_c(T)$ as a function of t^2 for all the samples except $x=3.0$ and 4.0. Data of Pb (Ref. 17) and the BCS curve are also shown for comparison.

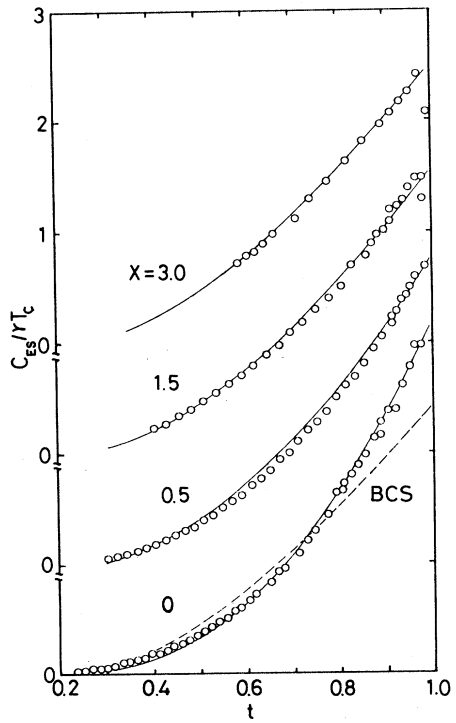

FIG. 5. $C_{ES}/\gamma T_c$ vs t for several samples. Solid and dashed lines are calculated from the α model (see the text) and the BCS theory, respectively.

tribution function. They assumed that the energy gap is independent of the energy and real, and that the normalized energy gap $\Delta(T)/\Delta(0)$ obeys the BCS theory. As a result, they showed that the superconducting electronic specific heat $C_{ES}/\gamma T_c = t[d(S_{ES}/\gamma T_c)/dt]$ could be calculated by use of only one adjustable gap parameter $\Delta(0)/k_B T_c$. The values of $C_{ES}/\gamma T_c$ are shown versus t in Fig. 5. The solid lines show the calculated results by the α model for our several samples. The temperature dependence for the samples with the small concentration x is much different from the BCS value (dashed line). The energy gap ratios $2\Delta(0)/k_B T_c$ used as adjustable parameters are shown versus x in Fig. 6. The concentration dependence of $2\Delta(0)/k_B T_c$ behaves similarly to that of the thermodynamic parameters.

In addition, the energy-gap ratios $2\Delta(0)/k_B T_c$ for Mo_6Se_8 and $Mo_6Se_7S_1$ were obtained directly by the tunneling experiments. Typical I versus V and (dV/dI) versus V curves are shown in Figs. 7(a) and 7(b). The I versus V curves near-zero bias indicate that junctions have considerable leakage current. The broad minimum of (dV/dI) versus V curves indicates the inhomogeneity of the junctions which might be caused by the destruction of the sample surface when the GaAs probe was moved onto the sample surface. The energy gap $\Delta(0)$ was estimated from the position of the minimum of the dV/dI versus V curve by considering the modification due to the thermal smearing. According to the BCS expression for (dI/dV) versus V, values of $\Delta(0)$ were given by reducing the voltages of the minimum position by 14% and 21% for Mo_6Se_8 and $Mo_6Se_7S_1$, respectively. The average gap ratios of many measurements are also shown in Fig. 6. The gap ratios obtained by the tunneling measurements are about 6%–14% larger than those estimated from the specific-heat analyses by the α model. This may be due to

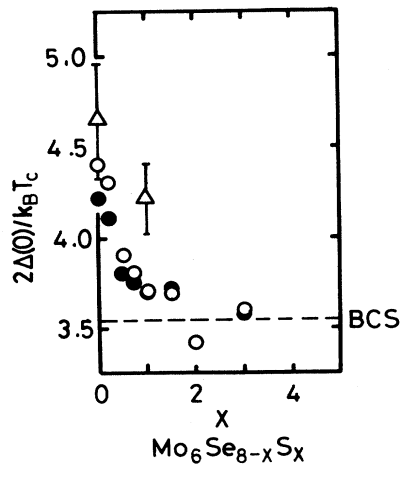

FIG. 6. Concentration dependence of $2\Delta(0)/k_B T_c$. Open and closed circles are obtained from the α model and Eq. (8), respectively. The dashed line shows the BCS value. Triangles represent the average values of the tunneling experiments. Many data exist within the bars.

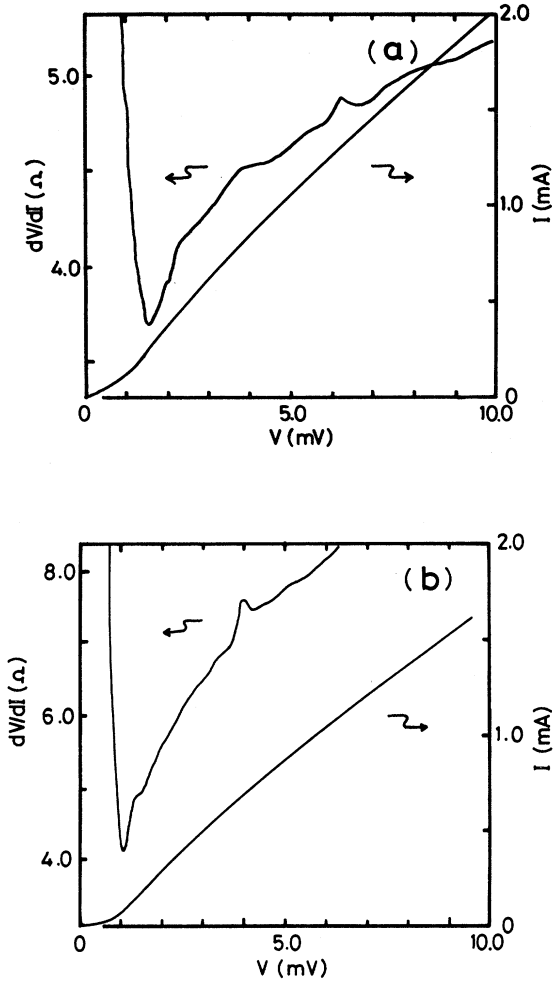

FIG. 7. Typical I vs V and dV/dI vs V curves. (a) $x=0$, $T=1.66$ K ($T_c=6.45$ K), $\Delta(0)=1.29$ meV, $2\Delta(0)/k_BT_c=4.7$; (b) $x=1.0$, $T=1.46$ K ($T_c=4.51$ K), $\Delta(0)=0.83$ meV, $2\Delta(0)/k_BT_c=4.2$.

the broad minimum of the (dV/dI) versus V curve. However, the trend of the concentration dependence is the same as the results of the specific-heat analyses.

IV. DISCUSSION

A. Electron-phonon interactions and average phonon frequency

The behavior of the thermodynamic parameters and the energy-gap ratio indicates that the electron-phonon

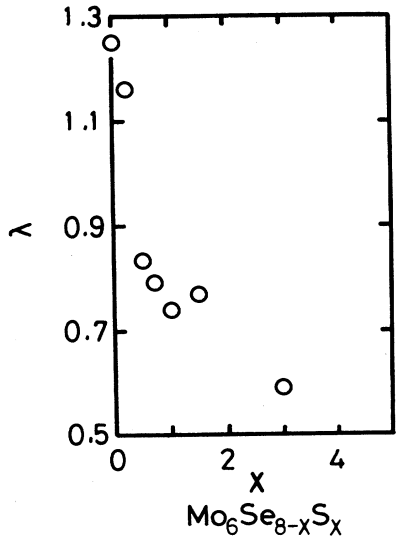

FIG. 8. Concentration dependence of the electron-phonon coupling constant, λ.

interactions changes with the concentration x. The electron-phonon coupling constant λ is estimated by use of the following expression proposed by Allen and Dynes[19] for the transition temperature of the strong-coupling superconductor:

$$T_c=f_1f_2\omega_{\ln}\times\exp[-1.04(1+\lambda)/(\lambda-\mu^*-0.62\lambda\mu^*)]/1.20\ , \tag{4}$$

where $\omega_{\ln}$ is an average phonon frequency given by

$$\omega_{\ln}=\exp[2\int_0^\infty d\omega\,\alpha^2F(\omega)\ln\omega/\lambda\omega]\ , \tag{5}$$

α^2 is the average electron-phonon interaction, $F(\omega)$ is the phonon density of states, and μ^* a Coulomb pseudopotential. f_1 and f_2 are correction factors for the strong-coupling interactions and can be equal to one except the case for very large λ. For the value of μ^*, the conventional value 0.1 is adopted. Here $\omega_{\ln}$ is determined as follows: The correction for the BCS ratio, $\Delta C/\gamma T_c$, by the strong electron-phonon interactions were expressed in the following approximate form by Marsiglio and Carbotte,[20]

$$\Delta C/\gamma T_c=1.43[1+53(T_c/\omega_{\ln})^2\ln(\omega_{\ln}/3T_c)]\ . \tag{6}$$

The value of $\omega_{\ln}$ obtained from the experimental values of $\Delta C/\gamma T_c$ and T_c is listed in Table III. These values of $\omega_{\ln}$

TABLE III. Average phonon frequency $\omega_{\ln}$ determined from Eq. (6), and the band density of states $N(0)$ determined by Eq. (11).

x	0.0	0.2	0.5	0.7	1.0	1.5	2.0	3.0	4.0
$\omega_{\ln}$ (meV)	5.8	5.5	8.4	8.9	10.0	7.5		10.1	
$N(0)$ (states/eV spin unit cell)	4.4	4.6	5.3	5.4	5.5	4.7		4.7	

are smaller than those of $A15$ compounds, 10.6 meV for Nb_3Ge and 10.8 meV for Nb_3Sn.[21] This result suggests that the lower-energy part of the phonon density of states becomes important for Chevrel phase compounds compared to $A15$ compounds. Thus the electron-phonon coupling constant λ is estimated by substituting the values of T_c and $\omega_{\ln}$ in Eq. (4). The values of λ are shown against the concentration x in Fig. 8. It is impossible to estimate the values of λ for $x=2.0$ and 4.0. Because the value of $\Delta C/\gamma T_c$ is 1.42 for $x=2.0$, then it is considered that this sample is in the weak-coupling limit. Furthermore ΔC for $x=4.0$ is impossible to obtain in the temperature range studied, as seen in Fig. 1(i). The values of the electron-phonon coupling constant change from the strong-coupling values to the weak one as the concentration x increases. The corrections to the other thermodynamic quantities of the strong-coupling superconductor were given by Marsiglio *et al.*[20] and Mitrović *et al.*[22] as follows:

$$H_c(0)^2/\gamma T_c^2=5.95[1-12.2(T_c/\omega_{\ln})^2(\omega_{\ln}/3T_c)]^{-1} \quad (7)$$

and

$$2\Delta(0)/k_BT_c=3.53[1+12.5(T_c/\omega_{\ln})^2\ln(\omega_{\ln}/2T_c)] . \quad (8)$$

These ratios calcualted by using the values of $\omega_{\ln}$ are also shown as closed circles in Fig. 3(b) and Fig. 6, respectively. As can be seen, the values obtained by the different procedures are in good agreement with each other.

Here, we consider the effects of the electron localization. The scale of the localization is expressed by the value of $\hbar/2\pi\varepsilon_F/\tau$, where ε_F and τ are the Fermi energy and the relaxation time of scattering, respectively, and can be estimated from the upper critical field measurement.[23] The electron localization is effective for $\hbar/2\pi\varepsilon_F\tau\sim1$ and then the value of μ^* is expected to be large. In our samples, however, the value of $\hbar/2\pi\varepsilon_F\tau$ is much smaller than 1. Furthermore, as mentioned above, the values of λ are reasonable ones when μ^* is taken to be 0.1. These results mean that the effects of electron localization can be ignored in our samples.

B. Superconducting transition temperature

The superconducting transition temperature depends exponentially upon the electron-phonon coupling constant λ and linearly upon the effective phonon frequency $\omega_{\ln}$ as seen in Eq. (4). Therefore the variation of λ is more effective in the change of T_c. In fact, there is a clear tendency that the higher T_c shows the higher λ, while the relationship between $\omega_{\ln}$ and T_c is opposite in our system, as seen in Table III.

According to McMillan,[24] the electron-phonon coupling constant can be decomposed as follows:

$$\lambda=N(0)\langle I^2\rangle/M\langle\omega^2\rangle , \quad (9)$$

where an average squared phonon frequency $\langle\omega^2\rangle$ is given by

$$\langle\omega^2\rangle=2\int_0^\infty d\omega\,\alpha^2F(\omega)\omega/\lambda , \quad (10)$$

$N(0)$ is the electronic density of states at the Fermi level,

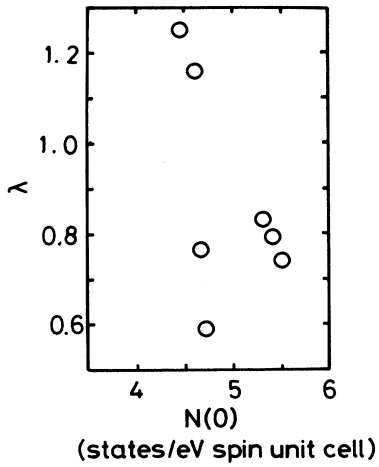

FIG. 9. Electron-phonon coupling constant λ as a function of the band density of states $N(0)$.

$\langle I^2\rangle$ is an average of the electron-phonon interactions over the Fermi surface, and M is the ion mass. The electronic density of states at the Fermi level is obtained from the electronic specific-heat coefficient

$$N(0)=3\gamma/2\pi^2k_B^2(1+\lambda) . \quad (11)$$

The values of $N(0)$ are also listed in Table III. Roughly speaking, the change in $\langle\omega^2\rangle$ is accompanied by a change in $\omega_{\ln}$. Then $\omega_{\ln}$ is used instead of $\langle\omega^2\rangle$. As the ion mass M, the molar mass $6M_1+8M_2$ is used, where M_1 and M_2 represent the mass of Mo and the averaged mass of $(Se_{8-x}S_x)/8$, respectively. The relationship between λ and $N(0)$, $\omega_{\ln}^{-2}$ and M^{-1} are shown in Figs. 9, 10, and 11, respectively. As can be seen in these figures, the value of λ does not depend on $N(0)$, while it depends linearly on $\omega_{\ln}^{-2}$. On the other hand, the value of λ seems to decrease with increasing M^{-1}, contrary to Eq. (9). Within the molecular crystal model, the mass used here represents only the effective mass of the acoustic translational phonon modes of the cluster. The effective mass

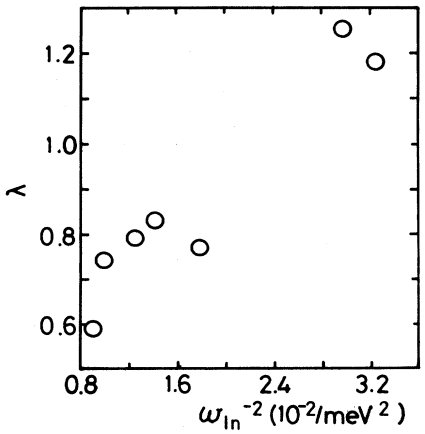

FIG. 10. Electron-phonon coupling constant λ as a function of $\omega_{\ln}^{-2}$.

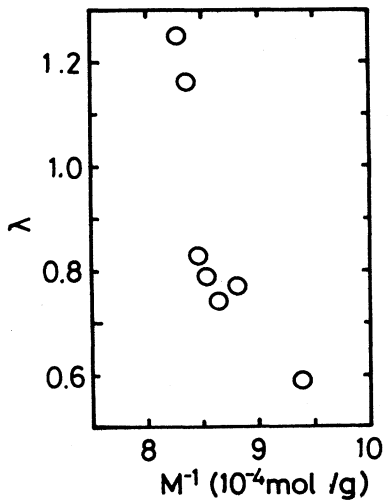

FIG. 11. Electron-phonon coupling constant λ as a function of M^{-1}.

for the torsional modes and the internal modes are represented by $\eta(M_1+4M_2)$ and $M_1M_2/(M_1+M_2)$,[9] respectively, where η is a constant related with length between chalcogen atoms. These effective masses are also not dependent on λ. As a result, the electron-phonon coupling parameter depends on the average phonon frequency $\omega_{\ln}$ and does not depend on the electronic density of states at Fermi level. This is different from results showing that λ is directly proportional to $N(0)$ for pure binary and pure ternary compounds.[3] The trend that the average phonon frequency shifts to lower energy, and then λ and T_c increase, was also observed in the high-T_c $A15$ compounds.[21]

C. Phonon mode softening and the electron-phonon interactions

1. Model for phonon density of states

First, on the basis of the molecular crystal model by Bader *et al.*,[7] the temperature dependence of the lattice specific heat is discussed. This model decomposes the phonon modes of the $Mo_6Se_{8-x}S_x$ crystal into three groups, reflecting its crystal structure which constitutes an ensemble of the quasirigid $Mo_6Se_{8-x}S_x$ units. The 42 phonon modes of a unit cell consist of 36 internal modes and six external modes. External modes are made of three translational acoustic modes and three torsional modes of the $Mo_6Se_{8-x}S_x$ unit. Lattice-dynamical calculations for Chevrel phase compounds were performed by Bader and Sinha[25] and compared with the molecular crystal model by Bader *et al.*,[7] where the hybridization between internal modes and external modes was pointed out.

The lattice specific heat at low temperatures studied includes only the contribution from the low-energy phonon excitations, and then the torsional and internal modes can be ignored because these modes lie in the high-energy region above 10 meV and have the almost flat dispersion as calculated by Bader and Sinha.[25] Therefore, only the three translational acoustic modes contribute to the low-temperature specific heat. The phonon density of states of these modes can be expressed by the Debye model with a cutoff energy of about 8 meV which was determined from the inelastic neutron scattering experiment for Mo_6Se_8 by Schweiss *et al.*[26] On the basis of this model, the lattice specific heat is calculated and compared to the experimental result in Fig. 1(a). However the anomalous temperature dependence of the specific heat cannot be explained as shown by the dashed curve in Fig. 1(a). Then, as previously pointed out by us for Mo_6Se_8 (Ref. 11), it becomes clear that the existence of lower-frequency modes should be considered for $0 \le x \le 1.5$.

The phonon model is modified by introducing low-lying phonon modes, $F_s(\omega)$, as follows:

$$F(\omega)=[2\varepsilon F_s(\omega)+(3-2\varepsilon)F_a(\omega)]/42 , \tag{12}$$

$$F_s(\omega)=3\omega^2/\omega_s^3 , \tag{13}$$

and

$$F_a(\omega)=3\omega^2/\omega_a^3 , \tag{14}$$

where ω_s and ω_a represent the cutoff energies of the low-lying soft-phonon modes and the translational acoustic-phonon modes, respectively, and ε means the ratio of low-lying phonon modes to the acoustic modes. We assume that the low-lying phonon modes are caused by phonon softening in the translational acoustic modes and expressed by Debye-like phonon modes. The experimental result for $x=0$ is first fitted by using the adjustable parameters ω_s, ω_a, and ε, where the γ value listed in Table I is used for the electronic contribution of the normal state. For samples of other concentration ($x>0$), the value of ω_s is fixed. Calculated results are also shown by the solid lines in Figs. 1(a) to 1(i). As can be seen, the agreement between experiments and the present model is quite excellent. The values of ω_s, ω_a, and ε are listed in Table IV. The concentration x dependence of ω_a is a reasonable one, because the mass of the cluster becomes lighter by substituting S for Se: ω_a is proportional to $M^{-1/2}$.

The amount of the low-lying phonon modes is expressed by ε in this model, and ε shows a similar concentration dependence to α as seen in Tables I and IV. Thus, it becomes clear that the anomalous specific heat is caused by the low-lying phonon modes with a characteristic energy of about 4 meV.

In the generalized phonon density of states obtained from the inelastic neutron experiments for Mo_6Se_8 by Schweiss *et al.*[8] the new small and broad peak around 5 meV, which did not appear at 297 K, was observed at 5 K. On the other hand, in Mo_6S_8 the low-lying phonon peak was not observed at both temperatures. In the case of Mo_6Se_8, this peak was attributed to the phonon softening in the TA $[1\bar{1}0]$ branch.[8] It is reasonable to consider that the low-lying phonon modes proposed in our model are just the softened ones because the ω_s value of 4 meV is in good agreement with the peak position of neutron experiment for Mo_6Se_8.

TABLE IV. Parameters ω_a, ω_s, and ε used for analyzing the normal state specific heat. ω_s is determined for $x=0$ and fixed for the other concentrations.

x	0.0	0.2	0.5	0.7	1.0	1.5	2.0	3.0	4.0
ω_a (meV)	8.4	8.4	8.5	8.5	8.6	8.6	9.0	9.0	10.0
ω_s (meV)	4.0	4.0	4.0	4.0	4.0	4.0	4.0	4.0	4.0
ε	0.110	0.088	0.059	0.050	0.020	0.020	0.0	0.0	0.0

2. *Electron-phonon interactions*

The electron-phonon coupling constant λ is expressed by

$$\lambda=2\int d\omega\,\alpha^2F(\omega)/\omega\ . \tag{15}$$

Thus, the low-energy part of $\alpha^2F(\omega)$ becomes dominant due to the denominator ω. Therefore the electron-phonon interactions are strongly influenced by the property of the low-energy part of the phonon density of states. The low-lying soft-phonon modes enhance $\alpha^2F(\omega)$ at low energies and make λ increase through Eq. (15). As seen in Fig. 12, the electron-phonon coupling constant λ is roughly proportional to the ε value which expresses the ratio of the low-lying soft-phonon modes to the acoustic modes. This relation indicates the importance of the low-lying soft-phonon modes in the electron-phonon interactions. This result is similar to the case of $A15$ compounds, in which the softening of $\alpha^2F(\omega)$ is related to the increase of T_c and λ.[21]

Structural phase transitions were observed in several Chevrel phase compounds which include the metal atom, Cu,[27] Ag,[28] and Ca, Ba, Sr, and Eu,[29,30] though the latter four compounds do not show superconductivity. The origin of the structural transition in the compounds including Cu and Ag atoms is the order-disorder transition of the metal atoms, but in the other compounds it remains unsolved yet. In $EuMo_6S_8$ studied by Decroux *et al.*,[31] the suppression of the structural transition under pressure causes a superconducting transition with rather high T_c of about 10 K. Moreover, in $PbMo_6S_8$ with the highest

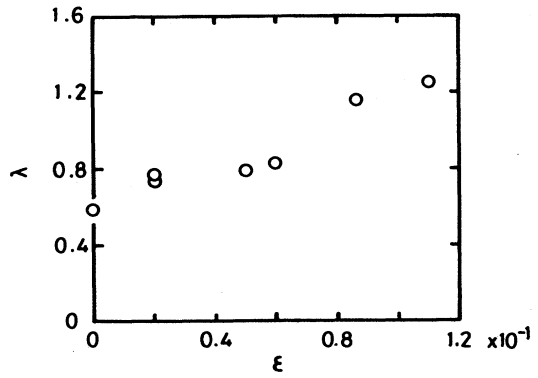

FIG. 12. Relationship between electron-phonon coupling constant λ and the ratio of the low-lying soft-phonon modes, ε.

T_c among Chevrel phase compounds, evidence of a structure instability at low temperature was observed in the neutron diffraction measurements by Jorgensen and Hinks.[32] These lattice instabilities would be related to the low-lying soft phonons observed in $Mo_6Se_{8-x}S_x$.

V. SUMMARY

The specific-heat measurements were performed on nine single crystals, $Mo_6Se_{8-x}S_x$, and tunneling measurements for two of them. The values of the thermodynamic parameters, $\Delta C/\gamma T_c$, $H_c(0)^2/\gamma T_c^2$, $-(dh_c/dt)_1$, $D(t)$, and $2\Delta(0)/k_BT_c$ obtained from specific-heat measurements behave similarly as the concentration x changes. These concentration dependences show that the electron-phonon interactions change from strong coupling to weak with increasing concentration. The values of $2\Delta(0)/k_BT_c$ obtained from the tunneling measurements also show a similar trend.

The electron-phonon coupling constant is estimated from $\Delta C/\gamma T_c$, according to the strong-coupling theories proposed by Marsiglio and Carbotte,[20] and Allen and Dynes.[19] The electron-phonon coupling constant changes monotonically from 1.25 to 0.6 with increasing concentration, where the Coulomb pseudopotential μ^* is taken to be 0.1

The change of T_c is dominated by that of the average phonon frequency $\omega_{\ln}$ through the electron-phonon coupling constant λ. The bare electronic density of states at the Fermi level $N(0)$ does not show the systematic change in this system. Therefore, the change of T_c is not dominated by $N(0)$.

Anomalous specific heat in the normal states is observed. The anomaly can be explained by the existence of the low-lying soft-phonon modes with the characteristic energy of 4 meV, which is consistent with the neutron experiment for Mo_6Se_8.[26] The electron-phonon coupling constant is proportional to the amount of the low-lying soft-phonon modes. Thus, it becomes apparent that these phonon modes play the important role for the electron-phonon interactions and thus the superconductivity in this system.

ACKNOWLEDGMENTS

The authors would like to thank Professor M. Tachiki, Professor T. Tsuzuki, Professor K. Noto, Professor T.

Fukase, Professor N. Toyota, Professor T. Satoh, Professor S. Maekawa, and Dr. M. Ikebe for useful discussions. The authors wish to thank Mr. T. Miura and Mr. H. Hariu for operating the furnace to prepare single crystals and Mr. K. Katagiri (Nippon Mining Co., Ltd.) for offering the GaAs wafer. They are also grateful to members of the Tohoku University Cryogenic Center and those of the machine shops of their institute for their technical support. This work was supported by the Grant-in-Aid for the Special Project Research on New Superconducting Materials from the Ministry of Education, Science and Culture, Japan. A part of this experiment was conducted at the High Field Laboratory for Superconducting Materials, Institute for Materials Research, Tohoku University, Japan.

---

*Present address: Institute for Materials Science, University of Tsukuba, Tsukuba, Ibaraki 305, Japan.

[1]Ø. Fischer, R. Odermatt, G. Bongi, H. Jones, R. Chevrel, and M. Sergent, Phys. Lett. **45**, A87 (1973).

[2]B. T. Matthias, M. Marezio, E. Corenzwit, A. S. Cooper, and H. E. Barz, Science **175**, 1465 (1972).

[3]B. Lachal, A. Junod, and J. Muller, J. Low Temp. Phys. **55**, 195 (1984).

[4]V. Sankaranarayanan, G. Rangarajan, R. Srinivasan, A. M. Umarj, and G. V. Subba Rao, Cryogenics **22**, 305 (1982).

[5]S. Maekawa and H. Fukuyama, J. Phys. Soc. Jpn. **51**, 1380 (1982).

[6]P. W. Anderson, K. A. Muttalib, and T. V. Ramakrishnan, Phys. Rev. B **28**, 117 (1983).

[7]S. D. Bader, G. S. Knapp, S. K. Sinha, B. P. Schweiss, and B. Renker, Phys. Rev. Lett. **37**, 344 (1976).

[8]B. P. Schweiss, B. Renker, and R. Flukiger, in *Ternary Superconductors,* edited by G. K. Shenoy, B. D. Dunlap, and F. Y. Fradin (North-Holland, New York, 1981), p. 29.

[9]F. J. Culetto and F. Pobell, Phys. Rev. Lett. **40**, 1104 (1978).

[10]U. Poppe and H. Wühl, J. Low. Temp. Phys. **43**, 371 (1981).

[11]N. Kobayashi, S. Higuchi, and Y. Muto, in *Superconductivity in d- and f-Band Metals,* edited by W. Buchel and W. Weber (Kernforschungszentrum Karlsruhe, Karlsruhe, 1982), p. 173.

[12]R. Chevrel, M. Sergent, and Ø. Fischer, Mat. Res. Bull. **10**, 1169 (1975).

[13]N. Kobayashi, K. Noto, and Y. Muto, J. Low. Temp. Phys. **27**, 217 (1977).

[14]W. A. Thompson and S. von Molnar, J. Appl. Phys. **41**, 5218 (1970).

[15]J. G. Adler and J. E. Jackson, Rev. Sci. Instrum. **37**, 1049 (1966).

[16]N. E. Alekseevskii, G. Wolf, S. Krautz, and V. I. Tsebro, J. Low Temp. Phys. **28**, 381 (1977).

[17]D. L. Decker, D. E. Mapother, and R. W. Shaw, Phys. Rev. **112**, 1888 (1958).

[18]H. Padamsee, J. E. Neighbor, and C. A. Shiffman, J. Low Temp. Phys. **12**, 387 (1973).

[19]P. B. Allen and R. C. Dynes, Phys. Rev. B **12**, 905 (1975).

[20]F. Marsiglio and J. P. Carbotte, Phys. Rev. B **33**, 6141 (1986).

[21]J. Kwo and T. H. Geballe, Phys. Rev. B **23**, 3230 (1981); K. E. Kihlstrom, D. Mael, and T. H. Geballe, *ibid.* **29**, 150 (1984).

[22]B. Mirović, H. B. Zarate, and J. P. Carbotte, Phys. Rev. B **29**, 184 (1984).

[23]M. Furuyama, N. Kobayashi, K. Noto, and Y. Muto, Jpn. J. Appl. Phys. **26**, Suppl. 26-3, 969 (1987); and (unpublished).

[24]W. L. McMillan, Phys. Rev. **167**, 331 (1968).

[25]S. D. Bader and S. K. Sinha, Phys. Rev. B **18**, 3082 (1978).

[26]B. P. Schweiss, B. Renker, E. Schneider, and W. Rechardt, in *Superconductivity in d- and f-Band Metals,* edited by D. H. Douglass (Plenum, New York, 1976), p. 189; see Ref. 13.

[27]R. Baillif, K. Yvon, R. Flükiger, and J. Muller, J. Low Temp. Phys. **12**, 231 (1979).

[28]Z.-H. Lee, K. Noto, and Y. Muto, J. Phys. Soc. Jpn. **52**, 2966 (1983).

[29]R. Baillif, A. Dunand, J. Muller, and K. Yvon, Phys. Rev. Lett. **47**, 672 (1981).

[30]B. Lachal, R. Baillif, A. Junod, and J. Muller, Solid State Commun. **45**, 849 (1983).

[31]M. Decroux, S. E. Lambert, M. S. Torikachvili, M. B. Maple, R. P. Guertin, L. D. Woolf, and R. Baillif, Phys. Rev. Lett. **23**, 1563 (1984).

[32]J. D. Jorgensen and D. G. Hinks, Solid State Commun. **53**, 289 (1985).